However, in ML_5 only one member of e'' mixes into the a_2'' HOMO. All d^0 MX_6 and MX_5 molecules studied here possess the VSEPR-mandated structures; namely, CrF_6 and WF_6 are found to be octahedral and VF_5 along with $TaCl_5$ are trigonal bipyramids. The situation for other ML_n complexes can be easily obtained in a qualitative fashion.

The valence orbitals of a d^0 MH_4 complex are presented on the right side of Figure 3. At the tetrahedral geometry there are again two empty d metal nonbonding orbitals. However, the t_2 HOMO already contains maximal d character. Thus, it is not surprising that TiH_4, which is a known compound,[92] has been found to be a local minimum (and in all likelihood the global minimum) at the tetrahedral geometry.[10,93] For a d^0 ML_2 system at the $D_{\infty h}$ geometry, the filled σ_u^+ orbital **43** has exclusively p character at the metal. One component of π_g, shown in **44**, will strongly mix into **43** upon bending to a C_{2v} structure. Thus, even in the highly ionic SrH_2 and BaH_2 molecules, bent rather than linear geometries are found.[9b] Furthermore, the calculated bending force constant varies inversely with the percentage of metal d hybridization for MX_2 molecules where M = Sr and Ba.[9a] The HOMO and LUMO for a trigonal planar d^0 MH_3 molecule are e' and e'', respectively (precisely analogous to e' and e'' for MH_5 on the left side of Figure 3). Although the e' set contains d character at the metal, upon pyramidalization e'' will mix into e', thus increasing the metal d hybridization. Jolly and Marynick[10] have found that ScH_3, TiH_3^+, and $TiMe_3^+$ all prefer pyramidal over planar structures at the HF level. We suspect that this will also be true when allowance is made for electron correlation.

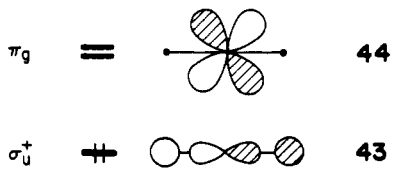

(92) (a) Breisacher, A.; Siegel, B. *J. Am. Chem. Soc.* **1963**, *85*, 1705. (b) Xiao, Z. L.; Hauge, R. H.; Margrave, J. L. *J. Phys. Chem.* **1991**, *95*, 2696.
(93) Thomas, J. R.; Quelch, G. E.; Seidl, E. T.; Schaeffer, H. F., III *J. Chem. Phys.* **1992**, *96*, 6857.

Acknowledgment. We wish to thank Drs. Arne Haaland, Jeremy Burdett, Odile Eisenstein, Oleg Charkin, Colin Marsden, Dennis Marynick, Fritz Schaeffer, and Monte Pettitt for many stimulating discussions. We gratefully acknowledge support from the Robert A. Welch Foundation, the donors of the Petroleum Research Fund as administered by the American Chemical Society, and the University of Houston's President's Research Enhancement Fund, and thanks are due to the National Science Foundation for a generous allocation of computer time at the Pittsburgh Supercomputing Center.

Supplementary Material Available: Coordinates (in Z-matrix form), total energies, and harmonic frequencies for **1-42** (45 pages). Ordering information is given on any current masthead page.

Interlayer Communication in Some Two-Dimensional Materials

Seeyearl Seong, Kyeong-Ae Yee, and Thomas A. Albright*

Contribution from the Department of Chemistry and Texas Center for Superconductivity, University of Houston, Houston, Texas 77204-5641. *Received September 18, 1992*

Abstract: Tight binding calculations with an extended Hückel Hamiltonian were used to probe interlayer bonding in four representative compounds. In V_2O_5, a straightforward interaction exists between the apical oxygen lone pairs and empty z^2 orbitals on vanadium in adjacent layers. There exists no covalent bonding between $Bi_2O_2^{2+}$ and WO_4^{2-} layers in Bi_2WO_6 at the prototype geometry. However, when the metal octahedra are tilted and the perovskite layer is shifted in its registry, two relatively strong bonds form between the out-of-plane oxygen atoms in the perovskite layer and bismuth. Here the interaction transfers electron density from the oxygen lone pairs to empty Bi–O σ^* orbitals. This, in turn, creates structural deformations within the $Bi_2O_2^{2+}$ layer. For $LiBiPd_2O_4$, we find covalent interaction between bismuth and palladium. Yet this does not appear to be the case in the topologically analogous $Pd_3P_2S_8$ structure. The reasons for the differences in covalent interaction are discussed in detail.

Introduction

From a geometrical point of view, layered or lamellar compounds[1] are inherently two-dimensional. A popular definition[1a] requires that they consist of electrically neutral layers held together only by van der Waals forces. Thus, layered compounds are easily cleaved, and the freshly exposed surfaces are relatively inert. Layer-type compounds have been extensively studied[1] in recent years, not only for their use as lubricants, etc., but also because of their highly anisotropic properties. Graphite and its fluorinated analog are perhaps the most well-known examples. In most compounds, the top and bottom layers of the "sandwiches" consist of anions only or, in some rare cases, of cations only.[1a,b] An interesting feature of many of these compounds is that their quasi-three-dimensional character can be gradually weakened or reinforced by intercalation with metal or organic radicals. Most frequently, electrostatic forces exist between the layer and the intercalate.

Trinquier and Hoffmann have suggested that weak covalent interlayer bonding exists between Pb atoms in adjacent layers in α- and β-PbO.[2] Likewise, weak interactions between Te atoms in certain MTe_2 phases have been found by Canadell, Whangbo, and co-workers.[3] It is our contention that this is a more general phenomena and that in many cases the remnants of covalent bonding can be found in layered compounds and intercalated

(1) (a) Hulliger, F. In *Structural Chemistry of Layer-Type Phases*; Levy, F., Ed.; D. Reidel: Dordrecht, 1976. (b) Bronger, W. In *Crystallography and Crystal Chemistry of Materials with Layered Structures*; Levy, F., Ed.; D. Reidel: Dordrecht, 1976. (c) Rouxel, J. In *Intercalated Layer Materials*; Levy, F., Ed.; D. Reidel: Dordrecht, 1979. (d) Grasso, V. *Electronic Structure and Electronic Transitions in Layered Materials*; D. Reidel: Dordrecht, 1986.

(2) Trinquier, G.; Hoffmann, R. *J. Phys. Chem.* **1984**, *88*, 6696.
(3) Canadell, E.; Jobic, S.; Brec, R.; Rouxel, J.; Whangbo, M.-H. *J. Solid State Chem.* **1992**, *99*, 189 and references therein.

0002-7863/93/1515-1981$04.00/0

materials. We have used a fragment molecular orbital perspective[4] to investigate this, since it oftentimes offers a convenient analytical solution. Fragment orbitals in layers which have been separated at an artificially long (chemically noninteracting) distance can be easily identified. Contraction of the layers to the experimental distance may cause some dispersion of the fragment orbitals. If a set of fragment orbitals in one layer is occupied and interacts with a set of empty fragment orbitals in adjacent layers, then that interaction will be stabilizing and some measure of covalency between the layers is established. This is simply the two-electron–two-orbital pattern for discrete molecules,[4b] and analogously the magnitude of the stabilization (covalent bonding) will depend directly upon the magnitude of the overlap turned on between the sets of fragment orbitals and inversely upon their energy difference. On the other hand, if both sets of fragment orbitals are filled, then any interaction will be repulsive—the analog of the two-orbital–four-electron problem. In this case, van der Waals or electrostatic forces alone will provide an attractive interaction between the layers. We have highlighted four examples to illustrate this interlayer communication. Tight binding calculations have been employed with an extended Hückel Hamiltonian.[5] Computational details have been provided in the Appendix.

V_2O_5

The chemistry of V_2O_5 has been actively investigated due to its role in the catalysis of hydrocarbons and SO_2.[6] It has also been used as a cathode material in lithium batteries[7] as a consequence of the facile intercalation and deintercalation of lithium. However, this is not true for larger cations, and this observation has led Murphy and co-workers to believe that weak interlayer bonding exists in V_2O_5.[7a,8] The structure[9] of V_2O_5 is shown in **1**. It is basically constructed of square pyramids sharing edges

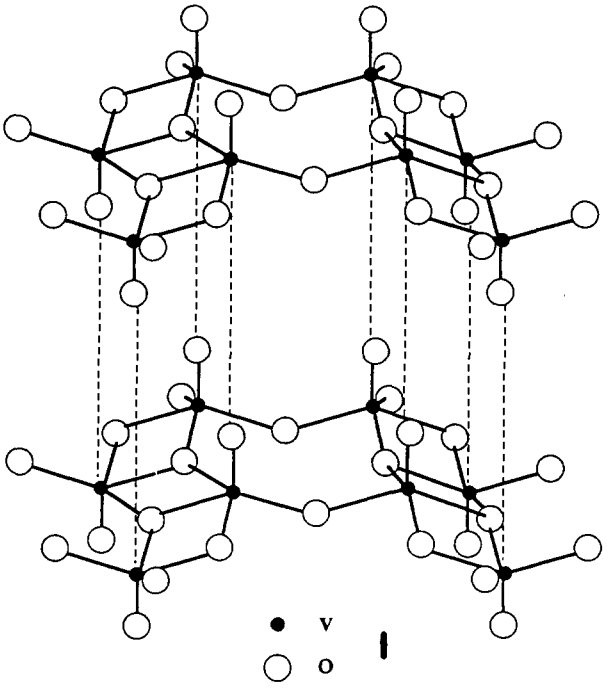

1

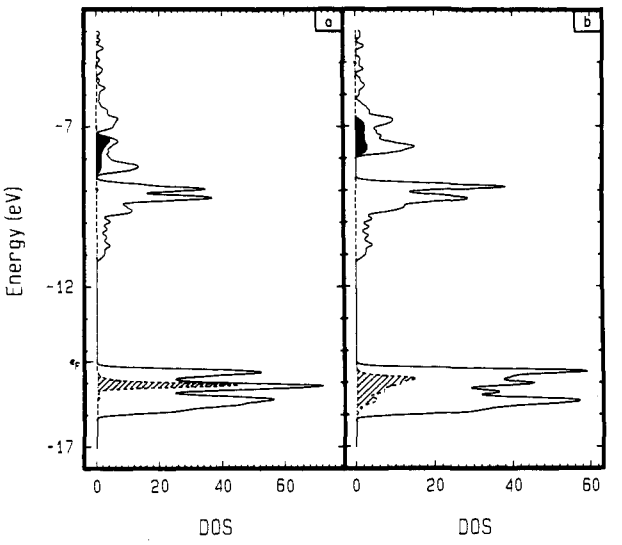

Figure 1. Density of states (DOS) for V_2O_5 when the distance between the apical oxygen atoms of one layer and the vanadium atoms of adjacent layers are set at 6.00 Å (a) and at the experimental distance, 2.79 Å (b). The projection of the apical lone pairs is given by the shaded area, and the projection for the z^2 hybrids by the darkened area. The top of the valence band is indicated by ϵ_F.

and corners. The four oxygen atoms in the base of the pyramid make up a nearly planar network. The vanadium atoms are displaced toward the apex of the square pyramid by 0.47 Å, which creates a very short V–O distance of 1.58 Å to the apical oxygen, whereas the average distance to the basal oxygens is 1.89 Å. The interlayer distance, as measured by the distance between the apical oxygen atoms in one layer and the vanadium atoms in an adjacent layer (the dotted line in **1**) is 2.79 Å.

The electronic structure of V_2O_5 has been extensively discussed elsewhere;[6,10] however, previous investigations have centered on spectroscopic properties and oxygen defects. We start our discussion by considering the well-known[4b,11] orbital splitting diagram for the isolated d^0 VO_5 square pyramid shown in **2**. At high

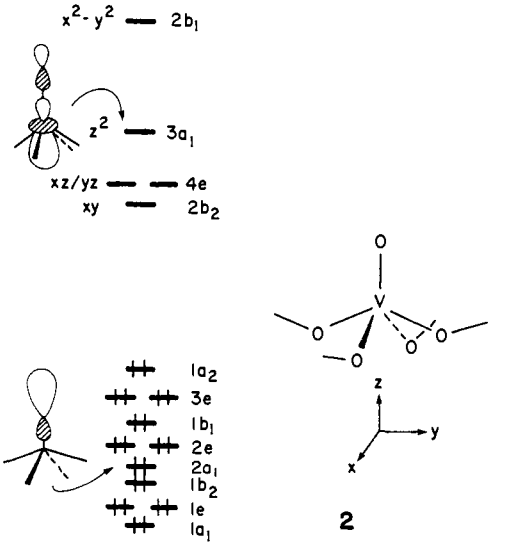

2

energy are the five empty metal d-based orbitals. The $3a_1$ orbital is explicitly drawn out. It is primarily z^2, and, importantly, it is hybridized out, away from the V–O apical bond, by the mixing

(4) (a) Hoffmann, R.; Fujimoto, H.; Swenson, J. R.; Wan, C.-C. *J. Am. Chem. Soc.* **1973**, *95*, 7144. Fujimoto, H.; Hoffmann, R. *J. Phys. Chem.* **1974**, *78*, 1167. (b) Albright, T. A.; Burdett, J. K.; Whangbo, M.-H. *Orbital Interactions in Chemistry*; John Wiley: New York, 1985.

(5) (a) Hoffmann, R. *J. Chem. Phys.* **1963**, *39*, 1397. (b) Hoffmann, R.; Lipscomb, W. N. *Ibid.* **1962**, *36*, 2179. (c) Whango, M.-H.; Hoffmann, R.; Woodward, R. B. *Proc. R. Soc. London, A* **1979**, *366*, 23.

(6) Ramirez, R.; Casal, B.; Uterera, L.; Ruiz-Hitzky, E. *J. Phys. Chem.* **1990**, *94*, 8960.

(7) (a) Murphy, D. W.; Christian, P. A. *Science* **1979**, *205*, 651. (b) Whittington, M. S. *J. Electrochem. Soc.* **1976**, *123*, 315.

(8) Cara, R. J.; Santoro, A.; Murphy, D. W.; Zahurak, S. M.; Fleming, R. M.; Marsh, P.; Roth, R. S. *J. Solid State Chem.* **1986**, *65*, 63.

(9) (a) Byström, A.; Wilhelmi, K. A.; Brotzen, O. *Acta Chem. Scand.* **1950**, *4*, 1119. (b) Bachmann, H. G.; Ahmed, F. R.; Barnes, W. H. *Z. Kristallogr.* **1961**, *115*, 110. (c) Enjalbert, R.; Galy, J. *Acta Crystallogr. Sect. C* **1986**, *42*, 1467.

(10) (a) Bullett, D. W. *J. Phys. C.: Solid State Phys.* **1980**, *13*, L595. (b) Lambrecht, W.; Djafari-Rouhani, B.; Lannoo, M.; Vennik, J. *Ibid.* **1980**, *13*, 2485. Lambrecht, W.; Djafari-Rouhani, B.; Lannoo, M.; Clauws, P.; Fiermans, L.; Vennik, J. *Ibid.* **1980**, *13*, 2503. Lambrecht, W.; Djafari-Rouhani, B.; Vennik, J. *J. Surf. Sci.* **1983**, *126*, 558. Lambrecht, W.; Djafari-Rouhani, B.; Vennik, J. *J. Solid State Commun.* **1981**, *39*, 257.

(11) Rossi, A.; Hoffmann, R. *Inorg. Chem.* **1975**, *14*, 365.

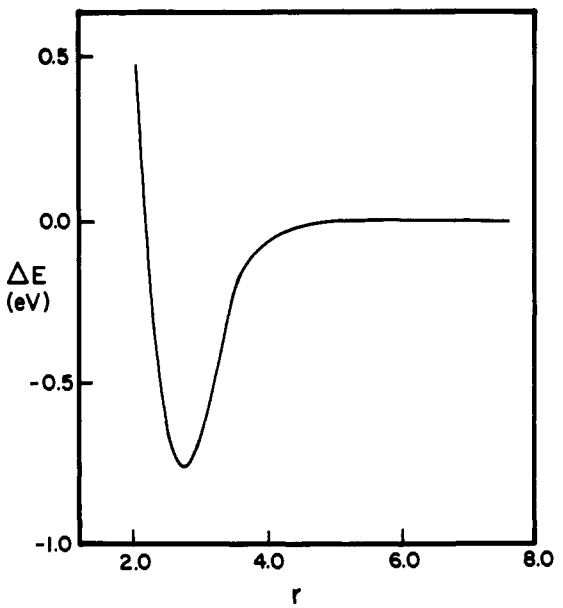

Figure 2. Variation of the interlayer distance in V_2O_5, r, versus the relative total energy (eV) per unit cell.

of metal s and z character. The highest occupied orbitals associated with a VO_5 square pyramid are oxygen lone pair combinations. One of these combinations, $2a_1$, is primarily associated with the apical oxygen atom and is hybridized in a direction away from the metal. The hybridization and moderate energies associated with the $2a_1$ and $3a_1$ orbitals make them ideal electron-donor and electron-acceptor functions, respectively, when V_2O_5 sheets are brought into close proximity.

Figure 1a shows the computed density of states (DOS) when the interlayer distance (the dotted line in **1**) was set at a chemically noninteracting value of 6.00 Å. The states from −14.4 to −16.1 eV correspond to the oxygen p region. The projection of the $2a_1$ orbitals to the total DOS is given by the shaded region. There is little dispersion since intralayer overlap of the $2a_1$ functions is quite weak. The darkened area from −7.2 to −8.5 eV corresponds to the projection of the $3a_1$ levels. The larger dispersion associated with $3a_1$ signals the fact that there is some (albeit small) interaction of z^2 in **2** with the basal oxygens. Variation of the apical oxygen to vanadium distance, r, in adjacent layers produces the potential energy curve shown in Figure 2. The optimal value of r was found to be 2.72 Å, in excellent agreement with the 2.79 Å found from the crystal structure.[9c] The agreement is probably fortuitous, given the approximate nature of the extended Hückel Hamiltonian. We find there to be 18.0 kcal/mol of stabilization per unit cell (4.5 kcal/mol per vanadium atom) when the layers are brought together from a long distance to the optimized one. One measure of interlayer covalent bonding that can be supplied is the Mulliken overlap population.[12] For reference purposes, the V–O overlap population to the intralayer apical and basal oxygens was computed to be 0.880 and 0.389, respectively. The interlayer V–O overlap population (to the apical oxygens) was 0.000 when the layers were separated by 6.00 Å, but it rises to 0.064 at the experimental geometry. Clearly some interlayer covalent bonding, given by the dashed line in **1**, exists.

Figure 1b shows the DOS and projections of the $2a_1$ and $3a_1$ orbitals when the interlayer distance is set to the experimental value. Notice in particular that the $2a_1$ projection (the shaded area) is considerably broadened from that in Figure 1a when the layers were separated by 6.00 Å. Some of the states are destabilized by repulsions from other filled orbitals, but the majority are stabilized. On the other hand, the majority of the $3a_1$ states (the darkened area) are destabilized. This is clear evidence for interlayer interaction between these two orbital groups. Since the $2a_1$-based orbitals are filled and $3a_1$ is empty, a net covalent bond, albeit weak, is formed between the layers. As a result of this interaction, 0.05 electrons are transferred from the apical oxygen atoms to the vanadium. We doubt that the situation we have described here is unique. A new polymorph of V_2O_5 exists[13] where the layers are strongly puckered. We suspect that a similar interaction occurs between the apical oxygens and vanadium atoms in adjacent layers. MoO_3,[14] $Mo_{18}O_{52}$,[15] $MoO_{2.8}F_{0.2}$,[16] and $Mo_2O_5(OH)$[17] represent another series where this interaction should exist.

Bi_2WO_6

Forty years ago Aurivillius discovered[18] a family of oxides with the composition of $Bi_2B_{n-1}M_nO_{3n+3}$. This was extended by Subbarao,[19] and now there are over 50 compounds in the group.[20] Many of these materials have been found to be ferroelectric,[20] and potential uses in memory storage and optical displays have been explored.[21] The structures consist of $B_{n-1}M_nO_{3n+1}$ perovskite slabs in which M is typically an early transition metal (e.g., Ti, Nb, Ta, Cr, W, and Fe), B is an electropositive atom (e.g., Na, K, Ca, Sr, Ba, Gd, La, B, Pr, Sn, Pb, and Bi), and n is the number of metal oxide layers. Sandwiched between the perovskite slabs is a Bi_2O_2 layer. The prototype structure for the Aurivillius phases has an I4/mmm tetragonal arrangement, shown from two perspectives in **3** for Bi_2WO_6. The bismuth atoms have square

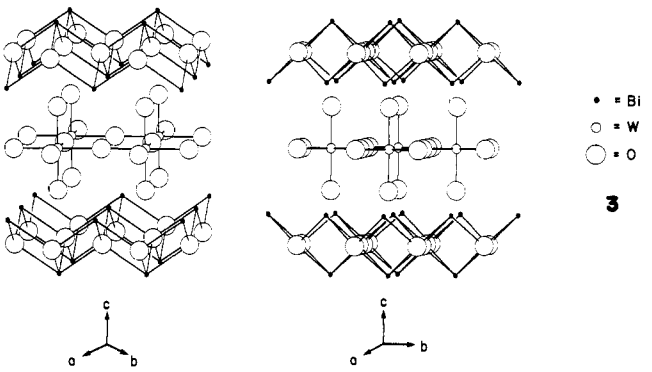

pyramidal coordination, and it is reasonable to assume a Bi(III) oxidation state; thus this layer can be considered as $(Bi_2O_2)^{2+}$, isoelectronic and isostructural to that in α-PbO. Clearly there will be strong electrostatic forces which hold the $(Bi_2O_2)^{2+}$ and WO_4^{2-} layers together. The actual structure of Bi_2WO_6 is much more complicated and has engendered some controversy.[22] In the most recent refinement,[22c] the most important displacements from the prototype can be described as follows: the perovskite layer is shifted by 0.35 Å in the a direction. The tungsten atom is displaced by 0.23 Å from the center of the octahedron toward an edge. The oxygen atoms in the Bi_2O_2 layer are laterally shifted

(12) Mulliken, R. S. *J. Chem. Phys.* **1955**, *23*, 1833, 1841, 2338, 2343.

(13) Cocciantelli, J. M.; Gravereau, P.; Doumerc, J. P.; Pouchard, M.; Hagenmuller, P. *J. Solid State Chem.* **1991**, *93*, 497.

(14) Kihlborg, L. *Ark. Kemi* **1963**, *21*, 357.

(15) Kihlborg, L. *Ark. Kemi* **1964**, *22*, 443.

(16) Pierce, J. W.; Vlasse, M. *Acta Crystallogr., Sect. B* **1972**, *27*, 158.

(17) Wilhelmi, K. A. *Acta Chem. Scand.* **1969**, *23*, 419.

(18) Aurivillius, B. *Ark. Kemi* **1949**, *1*, 463, 499; **1950**, *2*, 519; **1952**, *5*, 39. Aurivillius, B.; Fang, P. H. *Phys. Rev.* **1962**, *126*, 893.

(19) Subbarao, E. C. *J. Phys. Chem. Solids* **1962**, *23*, 665; *J. Am. Ceram. Soc.* **1962**, *45*, 166.

(20) For reviews, see: Newnham, R. E.; Wolfe, R. W.; Dorrian, J. F. *Mater. Res. Bull.* **1971**, *6*, 1029. Cross, L. E.; Pohanka, R. C. *Ibid.* **1971**, *6*, 939.

(21) Moulson, A. J.; Herbert, J. M. *Electroceramics: Materials, Properties and Applications*; Chapman and Hall: London, 1990. Jovalekic, C.; Atanasoska, L.; Petrovic, V.; Ristic, M. M. *J. Mater. Sci.* **1991**, *26*, 3553 and references therein.

(22) (a) Wolfe, R. W.; Newnham, R. E.; Kay, M. I. *Solid State Commun.* **1969**, 1797. (b) Gal'perin, E. L.; Erman, L. Ya.; Kolchin, I. K.; Belova, M. A.; Chernyshev, K. S. *Russ. J. Inorg. Chem.* **1966**, *11*, 1137. (c) Rae, A. D.; Thompson, J. G.; Withers, R. L. *Acta Crystallogr., Sect. B* **1991**, *47*, 870. (d) Varma, K. B. R.; Subbanna, G. N.; Guru Row, T. N.; Rao, C. N. R. *J. Mater. Res.* **1990**, *5*, 2718. Ramanan, A.; Gopalakrishnan, J.; Rao, C. N. R. *J. Solid State Chem.* **1985**, *60*, 376. (e) For the structure of Bi_2MoO_6, see: Teller, R. G.; Brazdil, J. F.; Grasselli, R. K.; Jorgensen, J. D. *Acta Crystallogr., Sect. C* **1984**, *40*, 2001.

in the a direction by 0.18 Å, and the WO_6 octahedra are rotated by 9.0° about the c axis. Finally, and what is important to the ensuing discussion, the octahedra tilt around the a axis by 10.3°. The basic structure is indicated in **4**. The tilting of the octahedra

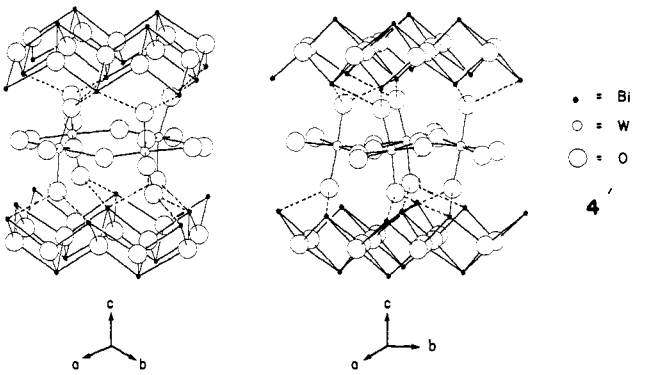

along with the lateral displacement of the perovskite layer brings two out-of-plane oxygen atoms in the WO_4 layer close to the bismuth atoms, as indicated by the dashed lines. These Bi–O distances, which are 2.91 Å in the prototype structure, now become 2.46 and 2.57 Å. The *average* (and there is considerable diversity to which we shall return later) Bi–O distance in the Bi_2O_2 layer is 2.33 Å. The structures for Bi_3TiNbO_9[23] and $Bi_4Ti_3O_{12}$,[24] the $n = 2$ and 3 members, respectively, of this family, display similar features.[24c]

To start our discussion of the bonding in the Aurivillius phases, the DOS plot of Bi_2WO_6 is presented in Figure 3 for the prototype structure. Below −14.0 eV are the W–O and Bi–O σ bonding orbitals along with the lone pairs on oxygen. From −10.1 to about −7.6 eV is the metal-centered "t_{2g}" set of orbitals associated with the tungsten octahedra. These constitute the lowest unfilled bands. Just above them lie Bi–O and W–O σ antibonding orbitals which are greatly dispersed. The shaded area in Figure 3 shows the projection of the lone pairs for the out-of-plane oxygen atoms in the perovskite layer. The lone pairs associated with the square pyramidal bismuth atoms are given by the sharp peak in the DOS at −14.0 eV. Notice that there is a small portion also associated with the out-of-plane oxygen lone pairs. This is a consequence of overlap between the two sets of orbitals. They combine to give bonding and antibonding combinations. The highest orbitals are primarily centered on bismuth with some oxygen lone pair character mixed in an antibonding fashion, as shown in **5**, for a portion of the Bi_2WO_6 unit cell. Since both sets of lone pairs

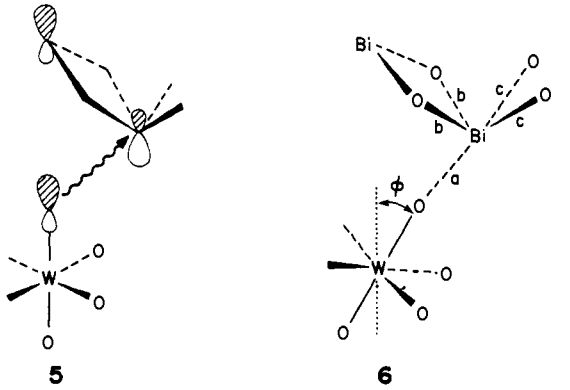

are filled, the net consequence of this overlap is repulsive. We,

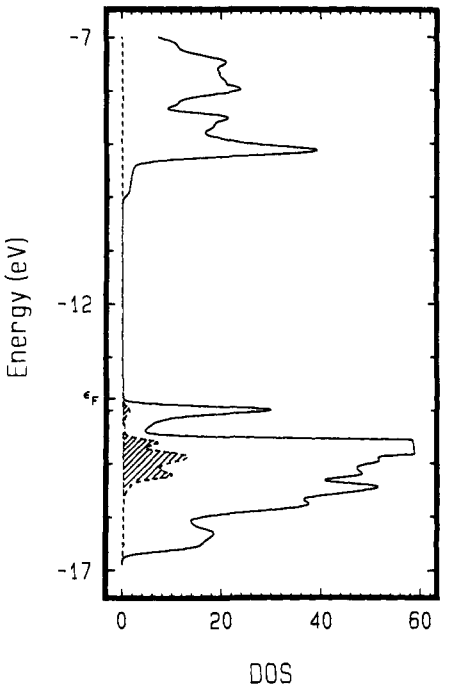

Figure 3. DOS for Bi_2WO_6 at the prototype structure. The shaded area indicates the projection of the lone pairs at the out-of-plane oxygen atoms. The Fermi level is indicated by ϵ_F. Notice that the peak at −14.5 eV has been truncated.

in fact, find this to be the case when we vary the interlayer distance for the prototype structure. One might think that tilting the octahedra about the a axis, ϕ in **6**, would increase the repulsion between the lone pairs. Indeed this is the case. At $\phi = 10.3°$, which corresponds to the amount of tilting in the experimental structure, the bismuth lone pair peak rises to −13.7 eV. However, the total Bi–O overlap population corresponding to a in **6** rises from 0.018 in the prototype structure (with $\phi = 0$) to 0.063. As shown diagramatically in **7**, Bi–O σ^* levels also mix into and stabilize the oxygen lone pair combinations. The result of these

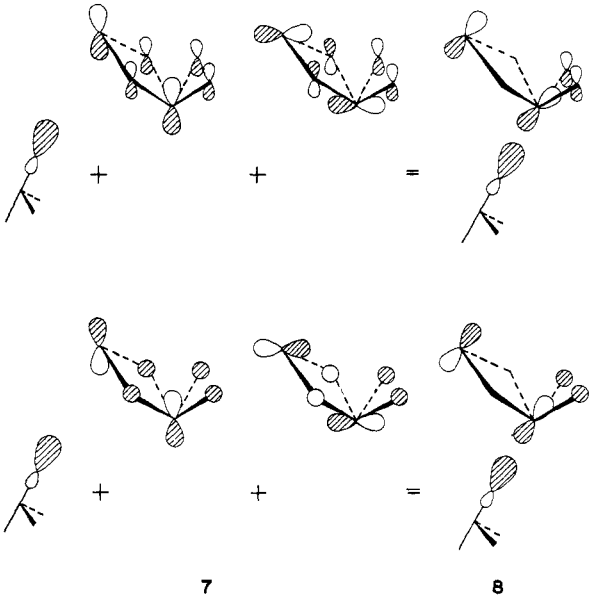

interactions, indicated in **8**, establishes a fifth bond to bismuth from the out-of-plane perovskite oxygens. **8** also indicates that the Bi–O bonds within the Bi_2O_2 layer and trans to the fifth interlayer Bi–O bond, labeled c in **6**, are preferentially weakened in comparison to the cis ones, b in **6**. At the prototype structure the Bi–O overlap populations were b = c = 0.231. At $\phi = 10.3°$ the corresponding values were b = 0.232 and c = 0.201. Electron

(23) (a) Wolf, R. W.; Newnham, R. E.; Smith, T. K.; Kay, M. I. *Ferroelectrics* **1971**, *3*, 1. (b) Thompson, J. G.; Rae, A. D.; Withers, R. L.; Craig, D. C. *Acta Crystallogr., Sect. B* **1991**, *47*, 174. (c) For $Sr_{0.9}Ba_{0.1}Bi_2Ta_2O_9$, see: Newnham, R. E.; Wolfe, R. W.; Horsey, R. S.; Diaz-Colon, F. A.; Kay, M. I. *Mater. Res. Bull.* **1973**, *8*, 1183. (d) For $SrBi_2Ta_2O_9$, see: Rae, A. D.; Thompson, J. G.; Withers, R. L. *Acta Crystallogr., Sect. B* **1992**, *48*, 418.

(24) (a) Dorrian, J. F.; Newnham, R. E.; Smith, D. K.; Kay, M. I. *Ferroelectrics* **1971**, *3*, 17. (b) Rae, A. D.; Thompson, J. G.; Withers, R. L.; Willis, A. C. *Acta Crystallogr., Sect. B* **1990**, *46*, 474. (c) Withers, R. L.; Thompson, J. G.; Rae, A. D. *J. Solid State Chem.* **1991**, *94*, 404.

density from the perovskite oxygen lone pairs is transferred to the Bi_2O_2 σ^* orbitals. In our calculations, 0.19 electrons per formula unit are transferred on going from the prototype to the tilted structure.

As outlined earlier, there are many other distortions besides the octahedral tilting one that occur in the structure of Bi_2WO_6. In the context of interlayer bonding, one other motion, namely the translation of the perovskite layer by 0.35 Å in the *a* direction, is quite important. A view roughly in the *ab* plane of one Bi_2O_2 layer along with the tungsten and out-of-plane oxygen atoms is presented in **9**. This lateral translation also creates short interlayer

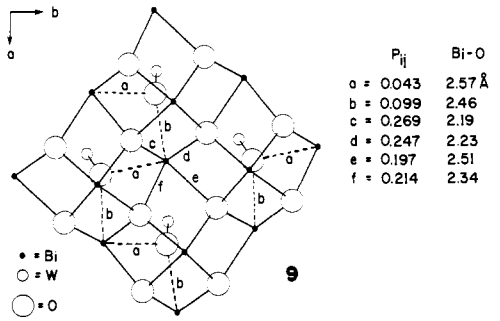

	P_{ij}	Bi-O
a =	0.043	2.57 Å
b =	0.099	2.46
c =	0.269	2.19
d =	0.247	2.23
e =	0.197	2.51
f =	0.214	2.34

9

Bi–O contacts which are labeled b in 9. Those formed by the octahedral tilting are designed by a. The electronic details associated with forming the b Bi–O bonds are identical to those given previously. Since the b bond is approximately positioned to be trans to the e and f (see 9) intralayer Bi–O bonds, electron donation from the filled oxygen lone pairs of the perovskite to Bi–O σ^* in the Bi_2O_2 layer should preferentially weaken e and f. Likewise, the formation of the interlayer a bond will weaken d and e. Therefore, one would expect the corresponding Bi–O bond lengths to vary in the order $c < d \sim f < e$. To model this situation we tilted the octahedra by 10.3° and shifted the perovskite layer by 0.35 Å in the *a* direction. All other geometrical parameters were fixed at those for the prototype structure. Note that in this calculation the interlayer Bi–O distances a and b approximately assume the experimental values while those for the c–f intralayer ones were all fixed at 2.31 Å. Therefore, the Bi–O overlap population differences within the layer give an indication of how the structure should distort, i.e., those bonds with larger overlap populations should become shorter and vice versa. The calculated Bi–O overlap populations P_{ij} along with the Bi–O distances in the experimental structure[22c] are listed in **9**. There is, in fact, a good correspondence between the calculated overlap populations and the Bi–O distances within the layer. Furthermore, the pattern predicted on the basis of the trans effect noted earlier is clearly in evidence here. The a and b Bi–O interlayer bonds are predicted to be considerably weaker than the intralayer ones. In a calculation at the experimental geometry the Bi–O overlap populations for a and b rise to 0.066 and 0.122, respectively. We find that 0.31 electrons per formula unit are transferred from the perovskite to the Bi_2O_2 layers on going from the prototype to the experimental structure. Just how much the covalent bonding between the layers is worth on an energetic basis is difficult to assess. As mentioned previously, neglecting the electrostatic component, the interlayer interaction is actually repulsive by 7.9 kcal/mol per formula unit upon going from a chemically noninteracting distance to the prototype structure. However, tilting the octahedra turns this into an attractive interaction by 7.3 kcal/mol per formula unit, and further distortion to the experimental structure offers an additional 1.3 kcal/mol stabilization. It is quite likely that our extended Hückel method underestimates the potential in this case. The situation we have covered here should certainly also apply to the other members of the Aurivillius family. It is also analogous to the electronic mechanism for interlayer Pb–Pb bonding in PbO,[2] and we suspect it is also present for the longer W–O separations in WO_2Cl_2[25] and the fourth, long Bi–O bond in $BaBiO_{2.5}$.[26]

(25) Jarchow, O.; Schröder, F.; Schulz, H. *Z. Anorg. Allg. Chem.* **1968**, *363*, 58.

$LiBiPd_2O_4$ and $Pd_3P_2S_8$

$LiBiPd_2O_4$ has a unique structure[27] in that all of the atoms are four coordinate with no less than three different coordination geometries. The basic structure is illustrated in **10**. The bismuth atoms are square pyramidal, and palladium is square planar. The

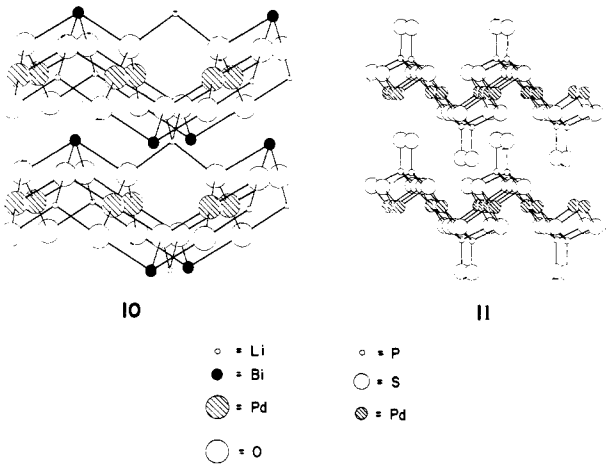

10 **11**

oxygen and lithium atoms both have tetrahedral coordination. Notice that there are two types of lithium atoms: those within the $BiPdO_4$ layers as well as those bridging the layers. The structure[28] of $Pd_3P_2S_8$, shown in **11**, is rather similar. It also has corrugated layers with palladium in a square planar environment. A slightly different perspective of both structures **12** and **13**

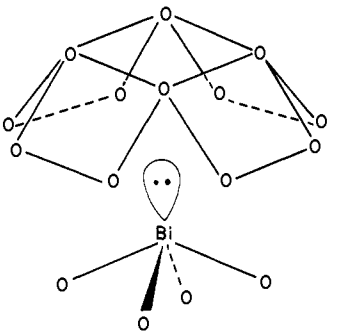

12

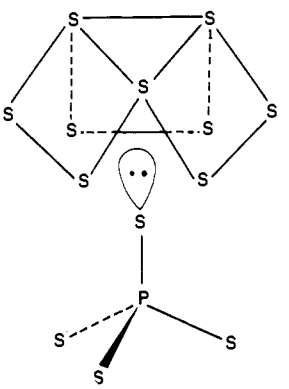

13

highlights a chief concern in the context of this work, namely that

(26) Lightfoot, P.; Hriljac, J. A.; Pei, S.; Zheng, Y.; Mitchell, A. W.; Richards, D. R.; Dabrowski, B.; Jorgensen, J. D.; Hinks, D. G. *J. Solid State Chem.* **1991**, *92*, 473.

(27) Laligant, Y.; LeBail, A.; Ferey, G. *J. Solid State Chem.* **1989**, *81*, 58.

(28) (a) Bither, T. A.; Donohue, P. C.; Young, H. S. *J. Solid State Chem.* **1971**, *3*, 300. (b) Simon, A.; Peters, K.; Peters, E.-M.; Hahn, H. *Z. Naturforsch.* **1983**, *38b*, 426.

in both structures there is a lone pair in one layer which extends into a cavity formed by the square planar palladium units in an adjacent layer. On the basis of the work in the previous sections, one would expect that donation of electrons from the lone pairs' density into empty orbitals within the cavity may produce a covalent interaction.

The splitting pattern for a square planar complex[4b] is given in **14**. Four metal orbitals, z^2, xz, yz, and xy, lie at low energies and are filled. The x^2-y^2 orbital lies at a higher energy. It is

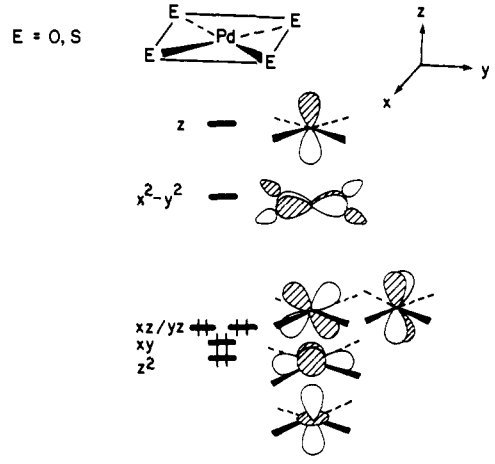

14

σ antibonding between the palladium and four surrounding atoms. Since the cavity is unoccupied, a suitable linear combination from the square planar units that comprise it could be used as an acceptor orbital for the lone pair on bismuth or sulfur atoms in **12** and **13**, respectively. However, since x^2-y^2 lies within the square plane, there will be little extension into the cavity. Therefore, interlayer overlap is quite small. Just above x^2-y^2 in energy is the palladium z orbital. There is sizable radial extension of this orbital within the cavity, and consequently it can act as an acceptor orbital.

Since our interest in this work is directed toward covalent rather than electrostatic interactions, let us consider a hypothetical $BiPd_2O_4^-$ system, isoelectronic and isostructural to $LiBiPd_2O_4$. The DOS plot calculated for a single layer of $BiPd_2O_4^-$ is shown in Figure 4a. The region from about −16.2 to −14.4 eV includes the Pd–O and Bi–O σ bonds along with the lone pair functions on oxygen. The z^2, xy, xz, and yz orbitals using the local coordinate system in **14** lie between −11.4 and −12.2 eV, and the empty x^2-y^2 levels are from −9.3 to −10.3 eV. What is germane to our discussion is that the bismuth lone pair projection is given by the shaded area in this figure, a well-defined peak at −14.2 eV. The empty palladium z orbitals lie in the region of −3 eV and are not shown in the figure. When a three-dimensional multilayer structure is computed at the experimental interlayer distance for $LiBiPd_2O_4$,[27] what has been anticipated in the previous discussion is, indeed, found. Namely, the bismuth lone pair states disperse toward lower energy and the palladium z orbital combinations of the requisite symmetry are dispersed upward in energy. The Bi–Pd overlap population was computed to be 0.051, and there is a 4.3 kcal/mol per formula unit stabilization for bringing the layers together to the experimental separation. It is interesting that the optimal interlayer distance was computed to be 0.41 Å shorter than the experimental one. This may well be an artifact of our extended Hückel method. The potential energy surface is soft in this region; only 1.3 kcal/mol per formula unit of stabilization is found for going from the experimentally observed to our optimal structure. When the palladium p atomic orbitals are deleted from the calculations, we find that the interlayer potential is repulsive. It now requires 0.6 kcal/mol per formula unit to bring the layers to the experimental distance. Thus, donation of electron density from the bismuth lone pairs to the palladium z orbitals creates an attractive interlayer potential. But the situation is somewhat more complicated than we have presented it to be.

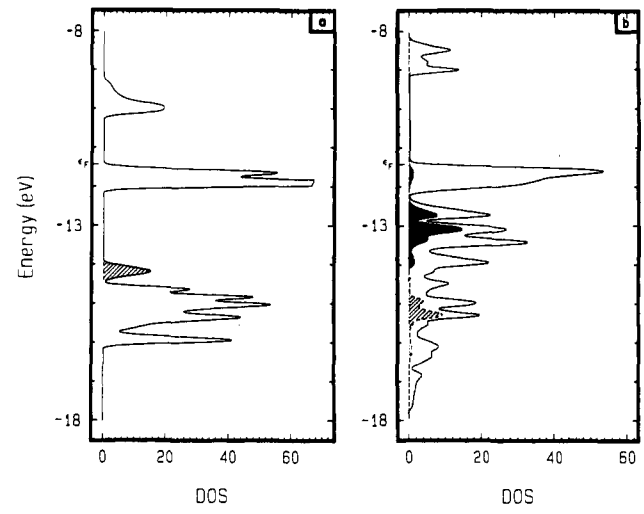

Figure 4. (a) DOS for a single layer of $BiPd_2O_4^-$. The shaded area indicates the projection of the bismuth lone pair, $3a_1$ in **15**. Notice that the peak at −12 eV lies off-scale. (b) The DOS for a single layer of $Pd_3P_2S_8$. The shaded area indicates the projection of the sulfur lone pair, $3a_1$, and the darkened area is the projection of the sulfur 2e set in **16**. In both plots the top of the valence band is indicated by ϵ_F.

An orbital interaction diagram for a BiO_4^{5-} unit interacting with a $Pd_4O_{12}^{16-}$ cavity is shown in **15**. The bismuth lone pair

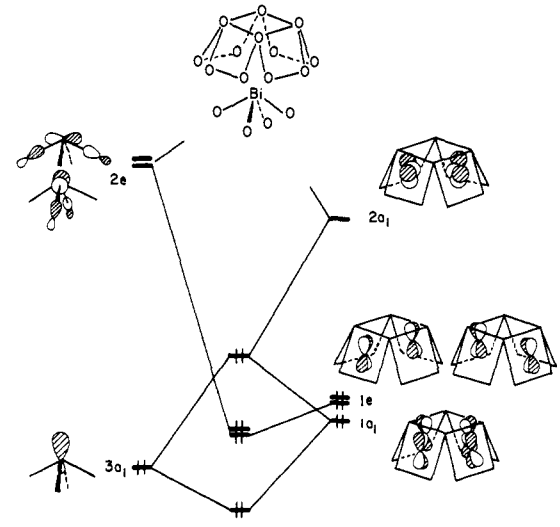

15

orbital $3a_1$ not only combines with the palladium z combination of a_1 symmetry, $2a_1$, but it also interacts with a combination of palladium xz/yz orbitals ($1a_1$).[29] The net result is a typical three-orbital pattern: the lowest orbital which is predominantly $3a_1$ is stabilized, $1a_1$ is left largely nonbonding, and the $2a_1$ orbital is destabilized. The relevant overlaps S_{ij} and overlap populations P_{ij} for these interactions are listed in Table I. The resultant orbital occupations n_i are also given. Notice that 0.088 electrons are transferred to what was formerly the empty $2a_1$ orbital. We also find that there is "back-donation" from the palladium xz/yz combination, 1e, to empty Bi–O σ antibonding orbitals, 2e. Inspection of the parameters in Table I shows that this interaction is weaker than that between $2a_1$ and $3a_1$; nonetheless, it still is significant; and 0.041 electrons are transferred to the 2e set in the bismuth oxide fragment.

The situation for $Pd_3P_2S_8$ might be expected to be quite similar to that discussed for $LiBiPd_2O_4$, yet it differs significantly in detail. At the experimental[28] interlayer distance the Pd–S interlayer

(29) There is also a palladium z^2 combination of a_1 symmetry which has appreciable radial extent into the cavity. However, the geometry is such that the overlap between this orbital and $3a_1$ is much smaller, and consequently there is much less interaction than that between $3a_1$ and $1a_1$.

Table I. Interaction Parameters for the $LiBiPd_2O_4$ and $Pd_3P_2S_8$ Systems

	$LiBiPd_2O_4$		$Pd_3P_2S_8$	
i/j	S_{ij}	P_{ij}	S_{ij}	P_{ij}
$1a_1/3a_1$	0.028	−0.002	0.019	−0.001
$2a_1/3a_1$	0.178	0.068	0.037	0.002
1e/2e	0.066	0.019	0.017	−0.001
n_{1a_1}	1.997		2.000	
n_{2a_1}	0.088		0.009	
n_{3a_1}	1.942		1.999	
n_{1e}	1.978		2.000	
n_{2e}	0.041		1.999	

overlap population was computed to be only 0.002.[30] Furthermore, the potential energy versus interlayer distance curve is totally repulsive. A diagram outlining the interaction between a PS_4^{3-} unit and a $Pd_3S_9^{12-}$ cavity is shown in **16**. The same basic

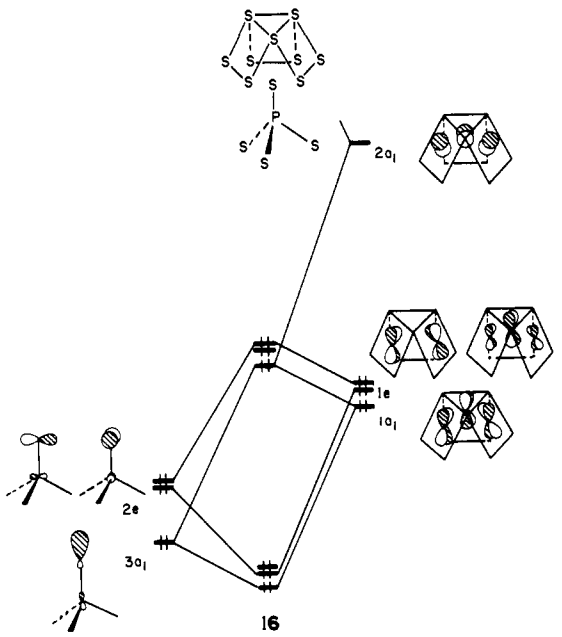

16

three-orbital pattern is found for $1a_1$, $2a_1$, and $3a_1$. The DOS plot for a single layer of $Pd_3P_2S_8$ is presented in Figure 4b. The shaded area indicates the projection of the $3a_1$ lone pairs on sulfur. They lie considerably lower in energy than the $3a_1$ bismuth lone pairs (Figure 4a). This is primarily a consequence of the greater electronegativity of sulfur. Therefore, the $3a_1$–$2a_1$ energy gap for $Pd_3P_2S_8$ is larger than that for $LiBiPd_2O_4$. Table I also shows that the overlap between $3a_1$ and $2a_1$ is much smaller in $Pd_3P_2S_8$. Thus, for energy gap and overlap reasons, the stabilizing $3a_1$–$2a_1$ component is quite weak in $Pd_3P_2S_8$. Notice from Table I that only 0.009 electrons are transferred to the $2a_1$ orbital. A second critical difference occurs in the 1e–2e interaction. For $LiBiPd_2O_4$ the 2e orbitals are empty, whereas in $Pd_3P_2S_8$ they correspond to filled lone pair combinations on sulfur. The projection of these states is indicated by the darkened area in Figure 4b. Since the 1e levels are also filled, this interaction is then a net two-orbital–four-electron repulsive one. Recall that the 1e–2e interaction in $LiBiPd_2O_4$ was stabilizing. We are left then with the notion that the interlayer force in $Pd_3P_2S_8$ is of the van der Waals type.

Conclusions

One analytical technique for investigating interlayer communication in solid-state materials is highlighted through four representative examples. Our tight binding calculations indicate that some interlayer covalent bonding exists in V_2O_5, Bi_2WO_6, and $LiBiPd_2O_4$. In each instance (and we suspect that this will be true in general) there is a lone pair orbital which has appreciable radial extent toward an adjacent layer. These lone pairs interact with and are stabilized by empty acceptor orbitals. One would normally expect that the lone pairs are associated with anions and the acceptors with cations. The situations in V_2O_5 and $LiBiPd_2O_4$ are two examples. However, in the Bi_2WO_6 case the acceptor orbitals are of the Bi–O σ^* type, concentrated on bismuth which would normally be considered an anion. We also find some evidence for donation from filled orbitals on palladium to empty bismuth centered orbitals in $LiBiPd_2O_4$. The Bi_2WO_6 example and certainly the other Aurivillius phases nicely illustrate that there can be structural distortions which accompany the donation of electron density to empty orbitals. Finally, $Pd_3P_2S_8$ offers a caveat. There may be too large an energy gap and/or too small an overlap between donor and acceptor functions. Furthermore, repulsive interactions between the layers may negate any covalent interactions. The examples given here concentrate in the metal oxide family; of course, these considerations apply equally well to other solid-state materials.

Acknowledgment. We thank the Robert A. Welch Foundation, the donors of the Petroleum Research Fund, administered by the American Chemical Society, the Texas Center for Superconductivity at the University of Houston (Prime Grant MDA 972-88-G-0002 from the Defense Advanced Research Projects Agency and the State of Texas), and the University of Houston President's Research Enhancement Fund for support of this work. We also thank the NSF for a generous allocation of computer time at the Pittsburgh Supercomputing Center.

Appendix

Tight binding calculations with an extended Hückel Hamiltonian[5] were used for all calculations. A modified version of the Wolfsberg–Helmholz formula was used.[32] The H_{ii} values and orbital exponents are listed in Table II and have been taken from previous work. The geometrical structures were taken from experimental work cited in the text. A 36K point set was used for V_2O_5 and Bi_2WO_6. The two-dimensional calculations on $BiPd_2O_4^-$ and $Pd_3P_2S_8$ used 45K and 44K points, respectively, while the three-dimensional calculations employed a 30K point set.

Table II. Parameters Used in the Extended Hückel Calculations

orbital	H_{ii} (eV)	ξ_1	ξ_2	C_1[a]	C_2[a]	ref
V 4s	−8.81	1.30				33
4p	−5.52	1.30				
3d	−11.00	4.75	1.70	0.4755	0.7052	
W 6s	−8.26	2.34				34
6p	−5.17	2.31				
5d	−10.37	4.98	2.07	0.6940	0.5631	
Pd 5s	−7.32	2.19				35
5p	−3.75	2.15				
4d	−12.02	5.98	2.61	0.5535	0.6701	
Bi 6s	−21.20	2.76				36
6p	−12.60	2.29				
O 2s	−32.30	2.28				37
2p	−14.80	2.28				
S 3s	−20.00	1.82				38
3p	−13.30	1.82				
P 3s	−18.60	1.60				39
3p	−14.00	1.60				

[a] Contraction coefficients used in the double-ζ expansion.

(30) We note that the calculated band gap is found to be 2.1 eV, which is in good agreement with experimental values of 2.2[28a] and 2.54 eV.[31]

(31) Folmer, J. C. W.; Turner, J. A.; Parkinson. B. A. *J. Solid State Chem.* **1987**, *68*, 28.

(32) Ammeter, J. H.; Bürgi, H.-B.; Thibeault, J. C.; Hoffmann, R. *J. Am. Chem. Soc.* **1978**, *100*, 3686.
(33) Kuâcek, P.; Hoffmann, R.; Havalas, Z. *Organometallics* **1982**, *1*, 180.
(34) Dedieu, A.; Albright, T. A.; Hoffmann, R. *J. Am. Chem. Soc.* **1979**, *101*, 3141.
(35) Tatsumi, K.; Hoffmann, R.; Yamamoto, A.; Stille, J. K. *Bull. Chem. Soc. Jpn.* **1981**, *54*, 1857.
(36) Whangbo, M.-H., private communication.
(37) Hoffmann, R. *J. Chem. Phys.* **1963**, *39*, 1397.
(38) Hoffmann, R.; Chen, M. M. L. *J. Am. Chem. Soc.* **1976**, *98*, 1647.
(39) Summerville, R. H.; Hoffmann, R. *J. Am. Chem. Soc.* **1976**, *98*, 7240.